A Motor-less and Gear-less Bio-mimetic Robotic Fish Design

C. Rossi, W. Coral, J. Colorado, A. Barrientos
Centre for Automation and Robotics
Universidad Politécnica de Madrid
Madrid, Spain
claudio.rossi@upm.es

Abstract— **In this paper, we describe our current work on bio-inspired locomotion systems using a deformable structure and smart materials, concretely Shape Memory Alloys, exploring the possibility of building motor-less and gear-less robots. A swimming underwater robot has been developed whose movements are generated using such actuators, used for bending the backbone of the fish, which in turn causes a change on the curvature of the body. This paper focuses on how standard swimming patterns can be reproduced with the proposed design, using an actuation dynamics model identified in prior work.**

I. INTRODUCTION

Actuation technology in robotics is basically centered on two kind of actuators: electric motors/servomotors and pneumatic/hydraulic actuators. In mobile robotics, the former is mostly used, with exceptions being e.g. large legged robots. The (rotatory) motion of the motors is transmitted to the effectors through gearboxes, bearings, belts and other mechanical devices in the case that linear actuation is needed. Although applied with success in uncountable robotic devices, such systems can be complex, heavy and bulky[1]. In underwater robots, propellers are most used for locomotion an maneuvering. Propellers however may have problems of cavitation, noise, efficiency, can get tangled with vegetation and other objects and can be dangerous for sea life.

Underwater creatures are capable of high performance movements in water. Thus, underwater robot design based on the mechanism of fish locomotion appears to be a promising approach. Over the past few years, researches have been developing underwater robots based on underwater creatures swimming mechanism [1], [2], [3], [4]. Yet, most of them still rely on servomotor technology and a structure made of a discrete number of linear elements, exceptions being the *Airacuda* by *FESTO*, which adopts pneumatic actuators, and the MIT fish [5]. Such fish has a continuous soft body, and a single motor generates a wave that is propagated backwards in order to generate propulsion.

Alternative actuation technology in active or "smart" materials has opened new horizons as far as simplicity, weight and dimensions. New materials such as piezo-electric fiber composite, electro-active polymers and shape memory alloys (SMA) are being investigated as a promising alternative to standard servomotor technology. The potential gain in weight and dimension would allow building lighter and smaller robots, and even devising soft-bodied robots [6].

In order to reproduce the undulatory body motion of fishes, smart materials appear to be extremely suited. In fact, over the last years, there has been an increasing activity in this field. Research in the field of smart materials for underwater locomotion is focused into mechatronics design and actuators control. As far as mechatronic design, much work is devoted to building hydrofoils using, e.g. piezo-electric fiber composite [7], embedding SMA wires into an elastic material such as silicone [8] or using SMAs as linear actuators [9]. Another important challenge is the control of such materials. Due to the relative novelty of smart materials technology, the literature and the know-how regarding their use is still weak. In the case of SMAs, excellent results have been achieved in [10], [11]. Parallel work carried out in the framework of this project is devoted to SMA control [12].

In this paper, we present our work on a swimming robot. The main characteristics of this robot are first, the concept of a continuous bendable structure of the robot actuated by a discrete number of (smart) actuators, and second, the complete lack of any standard mechanic parts and rotating actuators, i.e. a gear-less and motor-less robot.

Section II introduces a new mechatronic design which involves a continuous deformable structure, actuated by a discrete number of actuators made with SMA wires. In Section III we briefly describe swim patterns in fishes. Section IV presents the results of the simulations of the motion patterns, with the aim of demonstrating the feasibility of the concept. Finally, Section V concludes the paper with closing remarks on current and future work.

II. MECHATRONICS CONCEPT DESIGN

Fishes can swim bending their body in such a way to produce a backward-propagating propulsive wave. Such bending comes in different ways (see Figure 1). Anguilliform swimmers show a snake-like motion: their body can be divided into numerous segments from head to tail and can reproduce at least one complete wavelength along the body. Conversely, subcarangifor, carangiform and thunniform swimmers only bends roughly the second half of the body and the number of segments is reduced to one or two [13].

For our model, we have chosen to imitate the structure of subcarangiform swimmers because of the reduced number of

[1]Robotuna, a robot fish developed at MIT in 1994, had 2,843 parts controlled by six motors (source: MIT News, http://web.mit.edu/newsoffice/2009/robo-fish-0824.html)

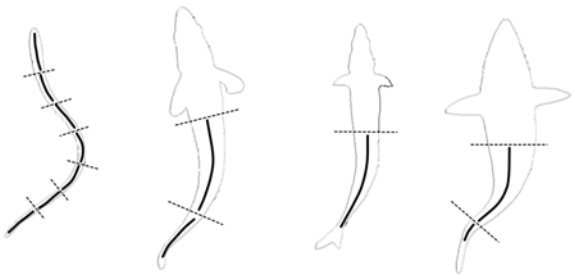

Fig. 1. Different kinds of undulatory swimming: from left to right: anguilliform, subcarangiform, carangiform, thunniform. (Figure adapted from [13].)

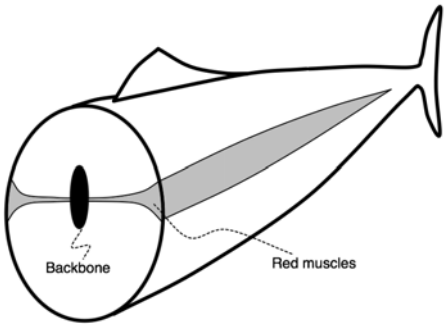

Fig. 2. Location of the red muscle fibres.

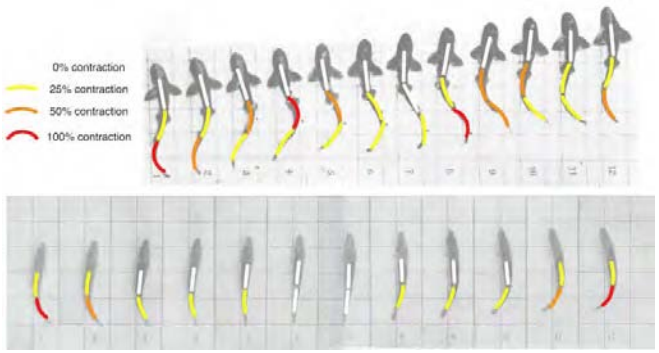

Fig. 3. Stills of the undulatory movement of body and tail segments (adapted from [15]). The proposed fish model can imitate both subcarangiform (top) and carangiform (bottom) swimming.

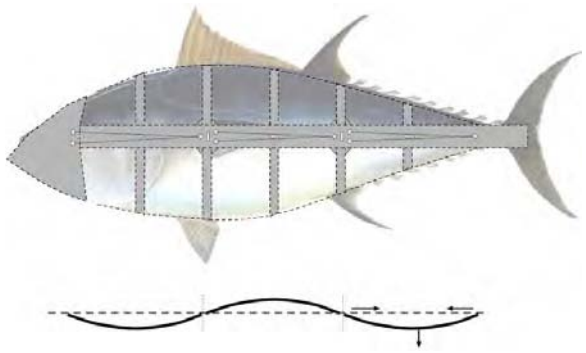

Fig. 4. Lateral and upper view of the deformable structure.

segments, which simplifies the study and the implementation of swimming patterns, while having enough degrees of freedom that allow different swimming modes to be reproduced (Fig. 3). Our fish model can also bend the head, which makes a total of three bendable segments (cf. Fig. 4).

Our robotic fish is formed by a continuous structure made of polycarbonate of 1 mm thickness, which represents the fish backbone and spines. This material has been chosen for its temperature resistance, impact resistance and flexibility. Additional supporting structure is employed to support the silicon-based skin that provides the three-dimensional shape to the robot. The overall length of the fish is 30 cm (not including the caudal fin).

Six SMA-based actuators are used to bend the body. Their length is $1/3$ body length (i.e. $8.5cm$, not counting the caudal fin and the head) and are positioned in pairs, parallel to the body in such a way to produce an antagonistic movement. Figure 5 shows a prototype of the structure and the location of the SMA wires. This arrangement imitates the red or slow-twitch muscles that fishes use during steady swimming (Fig. 2). As explained in [14], most fishes power swimming with their lateral musculature. Muscular contraction, and the mechanical properties of the passive components of the body combine to produce a wave of curvature that passes along the fish from head to tail. The body/tail wave generates net forward thrust. Lateral muscle fibres lengthen and shorten rhythmically during steady swimming. Low-tailbeat-frequency, sustained swimming is powered by slow-twitch aerobic muscle.

Thanks to this arrangement, the body segments can bend up to 28 degrees (angle β of Fig. 7), regardless the fact that SMA wires only contracts approximately a 4% of their length. The diameter size of the wires has been chosen as a trade-off between current consumption, pull force and contraction time. We have adopted a SMA with a diameter size of $150\mu m$ that has a pull force of 230 grams-force, a consumption of 250 mA at room temperature, and a nominal contraction time of 1 second. By increasing the input current and with a suitable control, contraction time can be accelerated up to 0.5 seconds, and strain can be increased to up to 6%, corresponding to a bending of 35°. Also, the V-shaped configuration of the wires, shown in Fig. 5, allows to double the pull force without a significant increase of power consumption.

A. Smart materials

SMAs are materials capable of changing their crystallographic structure due to changes in temperature: when an SMA wire is subjected to an electrical current, Joule resistive heating causes the SMA actuator to contract. We have chosen SMAs because they have the advantage that they work at low currents and voltages, are extremely cheap and easily available commercially. Nitinol, one of the most commercially available SMAs, is an alloy of nickel and titanium (NiTi). It is characterized by a high recovery stress ($> 500MPa$), low operational voltage ($4-5\ V$) and current,

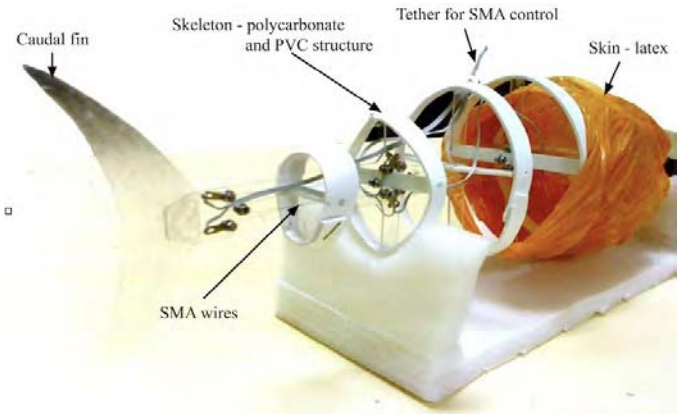

Fig. 5. Fish skeleton structure, with part of its latex skin.

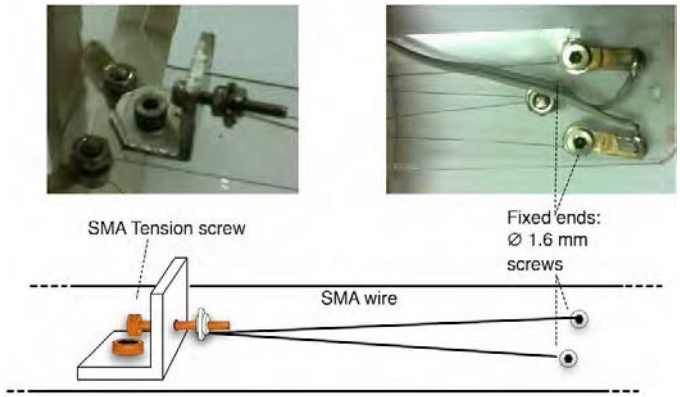

Fig. 6. Detail of the SMA arrangement, anchoring and tension regulation mechanics.

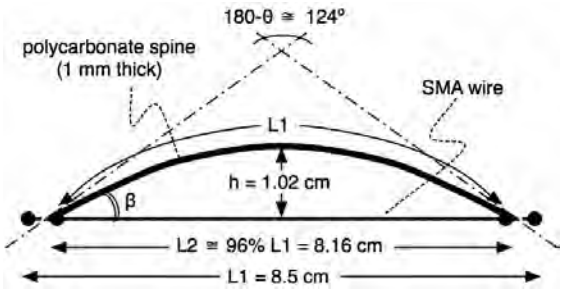

Fig. 7. Principle of the bendable structure. The SMA wires are parallel to the spine segment. As one contracts, it causes the polycarbonate strip to bend. $\theta \approx 56°$. The relationship is $L_2/L_1 = chord/arc = sin(\theta/2)/(\theta/2)$, where θ is the central angle of the circle sector, and $\beta = \theta/2 \approx 28°$. Note that antagonistic wire does not need to stretch.

a reasonable operational strain ($\approx 4\%$) and a long life (up to 10^6 cycles).

However, the behavior of SMAs is complex: the stress-strain relationship is non-linear, hysteretic, exhibits large reversible strains, and it is temperature dependent. Thus, the main criticism to their use is the difficulty of a precise control, although some authors have reported very good results [10],[11]. For this reason, we have employed them in a mechanism of underwater propulsion which is not demanding as far as precision.

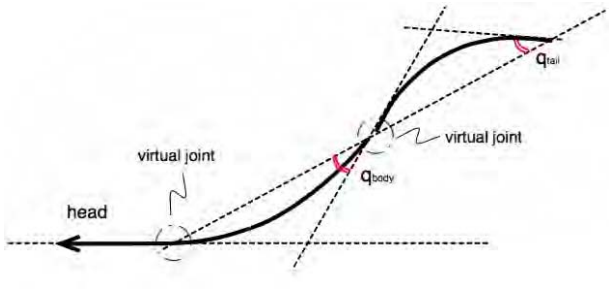

Fig. 8. Virtual joints approximation. A joint position q_j is equivalent to a bending angle of q_j w.r.t. the tangent of the previous segment's end, ($j \in \{body, tail\}$).

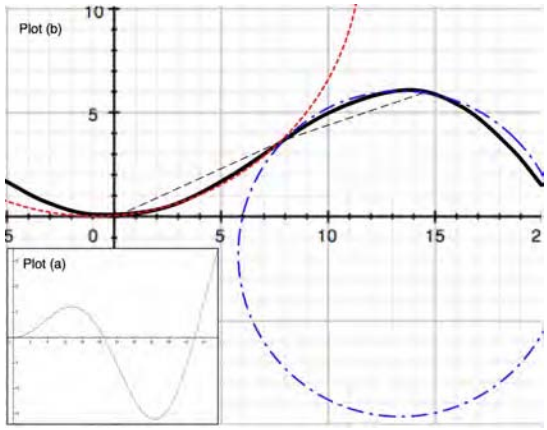

Fig. 9. Plot (a): $f_S(x,t)$ for $t = 0$ (Eq. 1). Plot (b): approximation of the swim function f_S with circles.

An important characteristics of SMAs is that they can also be used as sensors. In fact, once heated by applying a given current, one can measure their resistance and calculate the actual percentage of shrinking. This measurement is used as feedback for implementing position control.

B. Actuation dynamics identification and control

System identification has been performed on the prototype in order to design a low-level controller. The method for dynamics behavior identification consisted in measuring the electrical resistance of an SMA element. In fact, the resistance is being used as a form of temperature measurement. Measurements has shown that the hysteresis on the resistance curve is smaller than the hysteresis on the temperature curve. Hence, a linear approximation was feasible, and a first-order transfer function has been obtained from the measurements. The identified linear model allowed the development of a simple but efficient PID controller tuned using the Ziegler-Nichols methodology, which obtained errors of less than 1% in the resistance control, corresponding to a bending error of $0.69 - 5.99$ degrees. For more details about controller design and conducted experiments see [12].

III. SWIM PATTERNS

Swim patterns can be divided into two categories: periodic and aperiodic. Periodic swimming refers to cruise (steady) swimming and in-cruise turns, while aperiodic swimming

refers to sudden changes of directions (also referred to in the literature as "snap"-turns) and fast starts.

A. Steady swimming (cruise straight)

Pioneer work on swimming patterns is due to [15], [16], [17]. For steady forward swimming, the pattern can be described by the following equation:

$$y = f_S(x,t) = (c_1 x + c_2 x^2) sin(\frac{2\pi}{\lambda} x + \omega t) \quad (1)$$

where x is the longitudinal position with respect to the head of the fish and y is the lateral displacement. The c_1 and c_2 parameters define the wave amplitude, λ is the wave length, and ω the wave frequency.

In robotic systems, where the fish is implemented as a discrete number of elements, such wave form must be discretized in order to be reproduced. In the design proposed in [18] for example, one of the more advanced and best documented robot fish, the tail is discretized into four divisions of increasing length, and the curve is approximated by four segments. Following the methodology presented therein, the function governing the joints angle can be written as a time-dependent function q_j, where j is the joint index:

$$q_j(t) = a_j \cdot sin(\omega t + \phi_j), \qquad j = 1..number\ of\ joints \quad (2)$$

In our system, only the last two divisions are used for steady swimming ($j \in \{body, tail\}$). In order to analyze and simulate the system, we consider it as having two (virtual) joints that are governed with Equation (2). Thus, instead of a linear segment with a relative rotation of q_j, we have an arc whose tangent (the quantity referred to as "bending") at the end is equivalent to angle q_j (cf. Fig. 8). Since the actuators bend the structure into arcs, the curve (1) is approximated by circles, obtaining a smooth approximation with only two elements. Fig. 9 illustrates such approximation, and Fig. 3 illustrates the undulatory movement achieved by the body and tail segments.

B. Cruise-in turning

During steady swimming, smooth changes of direction, referred to as cruise-in turning, can be modeled as an asymmetry on the undulation with respect to the longitudinal axis. This can be modeled adding a bias function that defines a deflection curve:

$$y = f_S(x,t) + d(x) \quad (3)$$

On the practical side, this implies that the joint equation (2) becomes:

$$q_j(t) = a_j \cdot sin(\omega t + \phi_j) + b_j, \quad (4)$$

where the quantity b_j is related to the curvature radius of the turn, as we shall see in the next section.

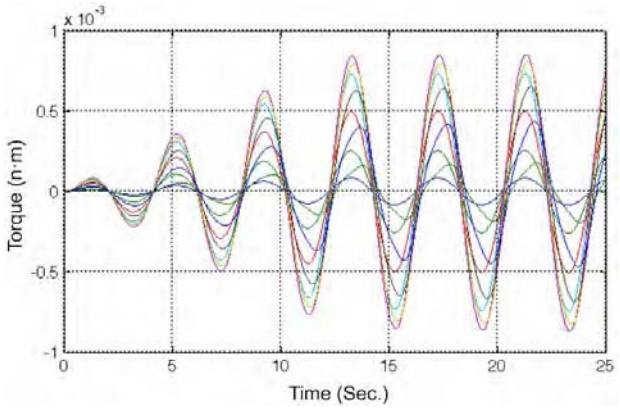

Fig. 10. Simulations results: torques at the joints corresponding to steady forward swimming ($a_{tail} = 0.54, a_{body} = a_{tail}/2, \phi_{tail} = -\pi/4, \phi_{body} = 0$, tail-beat frequency = $\pi/2$ Hz). Note the 4π startup period.

C. C-starts

This kind of aperiodic pattern is used for fast turns in response to external stimuli (e.g. for escaping from a menace or for capturing a prey). It comes into two ways: C-turns and S-turns, referring to the shape the fish takes during the maneuver. In real fishes such maneuvers take the order of milliseconds, and are activated by white (fast-twitch) muscles. It must be pointed out that SMA activation time is of the order of 0.5 to 1 seconds. This is why it makes sense to adopt them as *slow*-twitch (red) muscles for steady swimming. Nonetheless, in order to test the limits and possibilities of our concept and of SMA technology, we have implemented and simulated one of such "fast" stars, the C-shaped. In this paper we will limit the analysis of fast turning to qualitative considerations derived from the simulation results.

IV. SIMULATIONS

In order to assess the effectiveness of the proposed structure, we have conducted extensive numerical simulations, using the Bio-hydrodynamics Toolbox [19] for Matlab$^{(TM)}$ (BhT). Such tool provides a simple but thorough simulation tool. It allows to perform numerical simulation involving 2D motions of rigid bodies in an ideal fluid. BhT is based on the Lagrangian formalism (least action principle).

Since the toolboxs requires the model to be composed of articulated bodies, for the purpose of simulation the body of the fish had do be discretized into nine bodies (three for each fish body segment), with a mass proportional to the corresponding section of the fish body. The density of the material was set equal to the density of the water (neutral buoyancy) model's weight resulting of 200 grams.

The internal momenta acting on each body are shown in Fig. 10. Shape-changes between the bodies generate hydrodynamic forces and torques by which the bodies propel and steer themselves. Such a physical system based on both solid mechanics and fluid mechanics is called *fluid-structure interaction system*. Fig. 10 gives a useful insight about the

TABLE I

SUMMARY OF THE PERFORMANCES ON STEADY SWIMMING.

Maximum amplitude (a_{tail})	Tailbeat freq. (Hz)	Speed (m/s)	Speed (BL/s)
Half (0.25)	π/8	0.025	0.083
	π/4	0.025	0.083
	π/2	0.025	0.083
Nominal (0.49)	π/8	0.046	0.15
	π/4	0.048	0.16
	π/2	0.052	0.17
Overloaded (0.54)	π/8	0.093	0.31
	π/4	0.105	0.35
	π/2	0.114	0.38

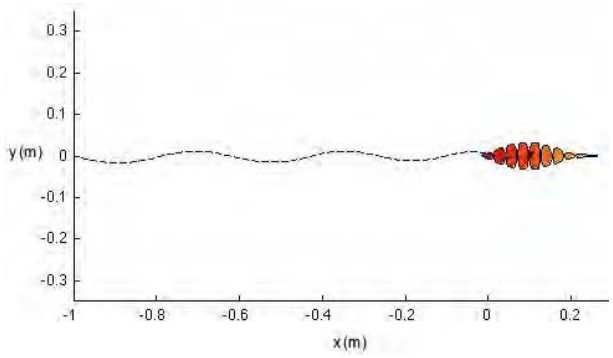

Fig. 11. Steady forward swimming ($a_{tail} = 0.54, a_{body} = a_{tail}/2, \phi_{tail} = -\pi/4, \phi_{body} = 0$, tail-beat frequency=π/2 Hz).

internal momenta generated under the fluid model of the Biohydrodynamics Toolbox, showing how symmetric torques evolution generates the steady forward swimming shown in Fig. 11. Maximum internal momenta of about $0.8 \cdot 10^{-3}$ Nm are required to generate the maximum bending amplitude of 31° (produced by the tail).

A. Steady swimming

Given the kinematic characteristics of our system, and based on the observation of fish swimming, the quantities corresponding to Eq. (2) are: $a_{tail} = 0.49, a_{body} = a_{tail}/2, \phi_{tail} = -\pi/4, \phi_{body} = 0$ for nominal SMA contraction (4%), and $a_{tail} = 0.54, a_{body} = a_{tail}/2, \phi_{tail} = -\pi/4, \phi_{body} = 0$ for overloaded SMA contraction (6%). Figure 11 shows an example of the trajectory followed by the fish. Table I reports the simulation results for steady swimming for various combinations of the maximum amplitude and frequency of the undulation (linear speed). For low amplitudes the speed achieved has no significant differences as far as tail-beat frequency.

Morphology parameters

Besides linear speed V, some other parameters are useful for evaluating quantitatively the soundness of the design. Speed expressed as body lengths (L) / second, $V_{BL} = V/L$ is reported in the last column of Table I. Good values are achieved for the largest amplitudes, which can be obtained overloading the SMA with a current up to 150%. Such value of course induces a further stress on the SMA, but it is worth noting that, due to the oscillatory nature of the actuation, high peaks are maintained only for short periods of time and are well bore by the material.

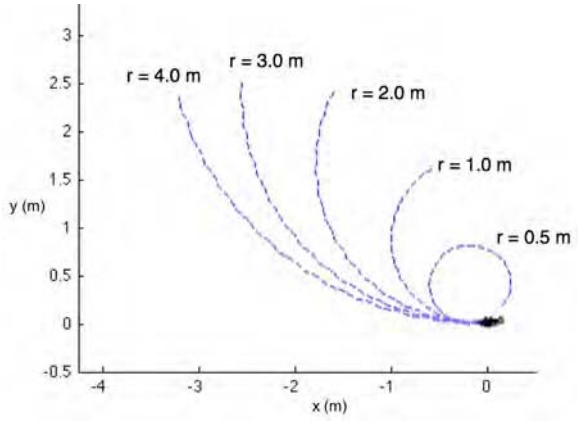

Fig. 12. Cruise-in turning. Labels refer to the desired turning radius (meters), corresponding (from left to right) to $b = 0.0375, 0.05, 0.075, 0.15, 0.3$.

Head swing factor S_h is the ratio between the tail tip oscillations and the head oscillations induced by body motion. It should range between 0.15 and 0.4, where higher values indicate that a large amount of energy is wasted because the head oscillates too much and has to push water to the sides. The best result achieved, with a fine tuning of the parameter ($a_{tail} = 0.49, a_{body} = 0.27, f = \pi/2\ Hz$, i.e overloaded amplitude), has been of 0.19.

Finally, the *Strouhal number* $S_t = f \cdot a_{tail}/V$, where f is the tail-beat frequency, refer to the wake vortexes generated by the fish tail. A normal value lays in the range 0.25 to 0.35. In the simulations, our robot fish can achieve, for optimal parameters' setting, a value of 0.26.

B. Cruise-in turning

For articulated bodies, it is easy to see that the bias b_j for each joint and the direction h of the last body w.r.t the first is $b = h/n$, n being the number of joints. On the other hand, for a circular arc of length L, the relationship between its radius r and the central angle θ is $r = L/\theta$. Since $h = \theta$ (from basic geometry), we have that

$$b_j = \frac{L}{n \cdot r}$$

In our case, $L = 0.3m$, $n = 2$ (virtual) joints, and the bias parameters b_j of Eq. (4) can be easily calculated given the desired turning radius r. Figure 12 shows the result for the cruise-in turning maneuver. The turning radius resulting from the simulations is well in agreement with the theoretical values calculated using the formula above. Using the same relationship, we can compute the minimum turning radius of the robot. Given that the maximum biases b_{tail} and b_{body} are equal to the maximum amplitudes a_{tail}, a_{body}, i.e. the oscillation is all at one side (e.g., 0 to a_{tail} instead of $-a_{tail}$ to a_{tail}) the minimum radius will be $r_{min} = \frac{L}{n \cdot b_{max}}$. This corresponds to a minimum theoretical turning radius of 0.83 meters. (In the simulations, turning radii of up to 0.5 meters have been achieved.) Finally, the maximum angular speed

Fig. 13. C-start sequence. The maneuver lasts 1 second. Note how for $t > 1.0$ the body starts to recover the straight position, but keeps on turning due to the inertia gained during the stroke.

obtained during such maneuvers is of 6 deg/s for turning radius of $0.5m$.

C. C-starts

In this maneuver all the three segments of the fish are bent, the head also taking part to the maneuver. A third virtual joint located on to the fish "neck" (right behind the head) also activates. A sharp turning C-start maneuver implies contracting the muscles on the same side in a synchronized way (i.e. $\phi_{tail} = \phi_{body} = \phi_{head}$). The velocity and amplitude of the contraction induces the turning angle. Figure 13 shows various stages of the best performing turn that can be obtained, corresponding to a SMA current overloading to increase the bending angle of 150%) for the three segments (a $375mA$ peak current pulse). From the figure, it can be appreciated that the fish turns of about 45° in one second during the start stroke.

After the starting stroke, the fish recovers the straight shape and begins steady swimming. During this period of time (approximately two tail beats) the fish holds the angular momentum generated with the initial stroke, and turns further 15°, escaping with a final angle of approximately 60°.

V. FINAL REMARKS AND CONCLUSIONS

We have presented our current work on bio-inspired locomotion for underwater robots. The objective of this work is to investigate new kinds of robots capable of changing their shape in a continuous way, and to investigate the use of active materials such as (but not limited to) SMAs as alternative actuation systems for such kind of robots.

The results of the numerical simulations confirm that the concept allows the robot to perform the main maneuvers according to the theory and models of fish swimming.

We would like to point out that the aim of our work is to experiment and elaborate on the concept of gear-less and motor-less robots. Compared to "classic" robotics theory, mathematical models, simulation tools, control techniques and general understanding regarding such concept are still in embryonic stage. However, it constitutes a promising concept that may lead to the next generation of robots.

The main advantage of this mechatronics design is its simplicity, extremely light weight and practically null volume of the actuators, at advantage of the available payload. Moreover, the actuators are absolutely silent and do not produce any vibration, a feature which can be exploited, e.g. in the observation of sea wild life since the robot would not disturb in any way (besides its presence). Current work is aimed at performing extensive experiments with the prototype in order to validate the results of the simulations.

In conclusion, we believe that smart actuators and flexible continuous structures can be a promising field for making alternative robots, that are simpler and lighter, and that can have interesting application domains.

REFERENCES

[1] H. Hu, "Biologically inspired design of autonomous robotic fish at Essex," in *IEEE SMC UK-RI Chapter Conference, on Advances in Cybernetic Systems*, pp. 3–8, 2006.

[2] J. M. Anderson and N. K. Chhabra, "Maneuvering and stability performance of a robotic tuna," *Integrative and Comparative Biolog*, vol. 42, no. 1, pp. 118–126, 2002.

[3] K. Morgansen, B. Triplett, and D. Klein, "Geometric methods for modeling and control of free-swimming fin-actuated underwater vehicles," *IEEE Transactions on Robotics*, vol. 23, no. 6, pp. 1184–1199, 2007.

[4] P. A. Vela, K. A. Morgansenand, and J. W. Burdick, "Underwater locomotion from oscillatory shape deformations," in *2002 IEEE Conference on Decision and Control*, 2002.

[5] P. Valdivia y Alvarado and K. Youcef-Toumi, "Design of machines with compliant bodies for biomimetic locomotion in liquid environments," *ASME Journal of Dynamic Systems, Measurement, and Control*, vol. 128, pp. 3–13, 2006.

[6] L. Cowan and I. Walker, "Soft continuum robots: The interaction of discrete and continuous elements," in *Artificial Life XI*, pp. 126–133, 2008.

[7] A. Ming, S. Park, Y. Nagata, and M. Shimojo, "Development of underwater robots using piezoelectric fiber composite," in *IEEE International Conference on Robotics and Automation*, 2009.

[8] Z. Wang, G. Hang, Y. Wang, J. Li, and W. Du, "Embedded sma wire actuated biomimetic fin: a module for biomimetic underwater propulsion," *Smart Materials and Structures*, vol. 17, no. 2, pp. 25–39, 2008.

[9] O. K. Rediniotis, L. N. Wilson, D. C. Lagoudas, and M. M. Khan, "Development of a shape-memory-alloy actuated biomimetic hydrofoil," *Journal of Intelligent Material Systems and Structures*, vol. 13, no. 1, pp. 35–49, 2002.

[10] Y. H. Teh, "An architecture for fast and accurate control of shape memory alloy actuators," *International Journal of Robotics Research*, vol. 27, no. 5, pp. 595–611, 2008.

[11] H. Meier, A. Czechowicz, and C. Haberland, "Control loops with detection of inner electrical resistance and fatigue-behaviour by activation of niti -shape memory alloys," in *European Symposium on Martensitic Transformations*, 2009.

[12] C. Rossi, A. Barrientos, and W. Coral, "SMA control for bio-mimetic fish locomotion," in *Proc- of the 7th International Conference on Informatics in Control, Automation and Robotics*, (Madeira, Portugal, June 15-18), pp. 147–152, 2010.

[13] M. Sfakiotakis, D. M. Lane, and J. B. C. Davies, "Review of fish swimming modes for aquatic locomotion," *IEEE journal of oceanic engineering*, vol. 24, no. 2, pp. 235–252, 1999.

[14] D. J. Ellerby, J. D. Altringham, T. Williams, and B. A. Block, "Slow muscle function of pacific bonito (sarda chiliensis) during steady swimming," *The Journal of Experimental Biology*, vol. 203, pp. 2001–2013, 2000.

[15] J. Gray, "Studies in animal locomotion," *Journal of Experimental Biology*, vol. 10, pp. 88–104, 1933.

[16] M. J. Lighthill, "Note on the swimming of slender fish," *Journal of Fluid Mechanics*, vol. 9, pp. 305–317, 1960.

[17] T. Wu., "Swimming of a waving plate," *Journal of Fluid Mechanics*, vol. 10, pp. 321–344, 1961.

[18] J. Liu and H. Hu, "Methodology of modelling fish-like swim patterns for robotic fish," in *Proceedings of the 2007 IEEE International Conference on Mechatronics and Automation*, 2007.

[19] A. Munnier and B. Pincon, "Biohydrodynamics toolbox," 2008. http://bht.gforge.inria.fr/.